Sufficient conditions for a period incrementing big bang bifurcation in one-dimensional maps

2011 Nonlinearity 24 2575

(http://iopscience.iop.org/0951-7715/24/9/012)

IOP PUBLISHING NONLINEARITY

Nonlinearity **24** (2011) 2575–2598 doi:10.1088/0951-7715/24/9/012

Sufficient conditions for a period incrementing big bang bifurcation in one-dimensional maps

V Avrutin, A Granados and M Schanz

IPVS, University of Stuttgart, Stuttgart, Germany

E-mail: Viktor.Avrutin@ipvs.uni-stuttgart.de, Albert.Granados@ipvs.uni-stuttgart.de and Michael.Schanz@ipvs.uni-stuttgart.de

Received 6 December 2010, in final form 22 June 2011
Published 2 August 2011
Online at stacks.iop.org/Non/24/2575

Recommended by Y G Kevrekidis

Abstract

Typically, big bang bifurcation occurs for one (or higher)-dimensional piecewise-defined discontinuous systems whenever two border collision bifurcation curves collide transversely in the parameter space. At that point, two (feasible) fixed points collide with one boundary in state space and become virtual, and, in the one-dimensional case, the map becomes continuous. Depending on the properties of the map near the codimension-two bifurcation point, there exist different scenarios regarding how the infinite number of periodic orbits are born, mainly the so-called period adding and period incrementing. In our work we prove that, in order to undergo a big bang bifurcation of the period incrementing type, it is sufficient for a piecewise-defined one-dimensional map that the colliding fixed points are attractive and with associated eigenvalues of different signs.

Mathematics Subject Classification: 37E05, 37G15

1. Introduction

In the context of piecewise-smooth dynamics, big bang bifurcations have been reported in the literature (see references below) as specific type of organizing centres in parameter space, where an infinite number of bifurcation curves issue from, separating existence regions of different periodic orbits with arbitrarily large periods. Typically, this codimension-two phenomenon has been detected in one-dimensional piecewise-smooth maps when globally investigating two-dimensional parameter spaces [1–3], although it is known that they occur also in higher-dimensional maps and flows.

The importance of these points bases on the fact that they organize the dynamics in the parameter space as all the possible periodic orbits existing in a neighbourhood of

such a point are 'created' there. In the cited works it was shown that there are several types of big bang bifurcations, which cause different bifurcation scenarios to occur in their neighbourhood.

Usually, these detections have been performed numerically and supported by analytical calculations, as no systematic procedures to detect and describe them have been reported until now. As these bifurcations can be observed in many systems in several fields, the question arises how to predict their occurrence and how to determine their type. The goal of our work is to prove sufficient conditions for one specific type of these bifurcations for one-dimensional piecewise-defined maps.

Based on experience, such a phenomenon seems to appear for piecewise-defined maps when, under certain conditions, two fixed points (or periodic orbits) collide simultaneously with the boundary. More precisely, consider an n-dimensional state space X split into two parts, X_ℓ and X_r, by a hypersurface Σ and two two-parameter diffeomorphisms $f_\ell(x; c_\ell, c_r)$, $f_r(x; c_\ell, c_r) : X \to X$. Suppose that $f_i, i \in \{\ell, r\}$, possesses a unique[1] invariant set given by a (stable) fixed point[2] x_i^* with real associated eigenvalues. Suppose also that for $c_\ell = c_r = 0$, both fixed points cross Σ transversally at the points $\tilde{x}_i^* \in \Sigma$[3]. Suppose also that, near $c_\ell = c_r = 0$, the position of the fixed point x_i^* is locally controlled by c_i. Let us then consider the piecewise-defined map

$$f(x) = \begin{cases} f_\ell(x; c_\ell, c_r) & \text{if } x \in X_\ell, \\ f_r(x; c_\ell, c_r) & \text{if } x \in X_r. \end{cases}$$

It is clear that, whenever one of these points crosses transversely the boundary, it undergoes a border collision bifurcation and the fixed point becomes virtual. Then, all initial values tend to the other fixed point or, eventually, to a two-periodic orbit with one iteration at each side of Σ. However, if both fixed points become virtual (increasing both parameters through $(c_\ell, c_r) = (0, 0)$) then, for values of (c_l, c_r) arbitrarily close to $(0^+, 0^+)$ it is possible to have periodic orbits of arbitrary period, with periodic points on both sides of Σ. That is, there may exist a *big bang* bifurcation at the origin of the parameter space $c_\ell \times c_r$. If one then encodes the periodic orbits depending on which side of Σ the consecutive iterates belong to, it is easy to see that the possible symbolic sequences of the periodic orbits mainly depend on the sign of the eigenvalues of the fixed points associated with the eigendirections pointing to Σ. An explicit description of which symbolic sequences are possible and which are not, for every case, remains an open problem.

As mentioned above, in this work we will restrict ourselves to one-dimensional maps f such that both colliding fixed points are stable (f_ℓ and f_r are contractive near $x = 0$ if c_ℓ and c_r are small). In that case, one has $X = \mathbb{R}$, $\Sigma = \{0\}$ (up to translation) and f becomes a map with a single discontinuity at $x = 0$. The distance between the fixed points and the boundary is controlled by the offsets c_ℓ and c_r at the origin, and the sign of the eigenvalues of the fixed points is, obviously, given by the slopes of f_ℓ and f_r near $x = 0$ for c_ℓ and c_r small.

Then, regarding this sign one can consider two different interesting cases: positive–positive (increasing–increasing) and positive–negative (increasing–decreasing)[4] for

[1] We consider it unique for simplicity. Obviously, everything in what follows remains the same if both fixed points can be isolated from other invariant sets in a certain neighbourhood.

[2] For simplicity, we assume them to be fixed points, considering an appropriate iterated function everything can be argued similarly also for periodic orbits.

[3] Note that, for $n > 1$, we do not assume that $\tilde{x}_\ell^* = \tilde{x}_r^*$. Therefore, in general, f would not necessary have to be continuous at the codimension-two bifurcation point.

[4] Recall that we are dealing in this work with maps contractive on both sides. Then, the decreasing–increasing case is equivalent to the increasing–decreasing one. For the decreasing–decreasing one, only a two-periodic orbit or one or two fixed points are possible.

which the bifurcation scenarios near the codimension-two bifurcation point are very different.

The bifurcation scenarios for these two cases were first studied using the offsets as a particular parametrization of a linear piecewise-defined map by Leonov in the late 1950s ([4], see also [5]). There, using direct computations, both scenarios were described, and have been later called *period adding* (increasing–increasing) and *period incrementing* (increasing–decreasing) [1].

Later, it was shown that similar maps were obtained as first return maps of n-dimensional flows ($n \geqslant 3$) near a double homoclinic bifurcation. In this context, this type of (contracting) map has been intensively studied [6–15], both near the codimension-two bifurcation point and far away from it.

For the contractive case, a first study of the codimension-two bifurcation point in a two-dimensional parameter space was performed in [6]. It was there mentioned in a footnote that going through a certain region in this space one could find an infinite number of periodic (and also aperiodic) orbits and that this region shrinks infinitely to the origin of the parameter space, the big bang bifurcation point. One month later, it was stated in [7] a first relation between the possible symbolic sequences of the periodic orbits near the codimension-two bifurcation point, their rotation numbers and their connection to the Farey numbers. This point was called *gluing bifurcation*, as the periodic orbits created there were obtained by 'gluing' other periodic orbits. This was finally proved in [8] for a contraction ratio less than $\frac{1}{2}$ and later in [16] for the pure contracting case.

However, in none of these works was the sign of the eigenvalues considered and, therefore, no distinction between the different bifurcation scenarios was taken into account. This in fact represents the main difference between a gluing bifurcation and the codimension-two bifurcation point that, following [1], we refer to here as the big bang bifurcation. While the last one is characterized by an infinite number of bifurcation curves issuing from the point thereby separating periodic orbits with arbitrarily large periods, the first one refers to the fact that two periodic orbits are glued, although maybe an infinite number of times through successive gluing. This implies, for example, that for the decreasing–decreasing case (see footnote 4) a gluing bifurcation occurs creating a two-cycle, but is not a big bang bifurcation as the two colliding fixed points and the two-periodic orbit are the unique invariant objects that one can find near the codimension-two bifurcation point.

A long time after Leonov, in the context of the double homoclinic bifurcation, the scenario for the increasing–increasing case (period adding) was first described for a quadratic piecewise-defined map at the same time in [9, 13], and later studied in more detail in [12, 14] using direct computations for low periods and renormalization techniques. There, it was shown that the infinite number of periodic orbits emerging from the origin of the parameter space are created by 'gluing' them and adding their periods. More recent studies [1–3] have shown, using direct computations and numerical simulations, that this phenomenon seems to appear for other piecewise-defined maps.

On the other hand, very rigorous works [17–23] also gave classification, properties and the sets of periods of the possible periodic orbits using kneading invariants. This was done for expansive increasing–increasing maps (also called Lorenz-like maps) for which an explicit list of the possible periodic orbits is still missing when a similar parametrization controlling the offsets is used.

The periodic orbits emerging from the origin of the parameter space for the increasing–decreasing case were first described also in [4] ([5]) for a piecewise-linear map. The resulting bifurcation scenario was proven in [10] for a particular parametrization of a contractive quadratic piecewise-defined map. This was achieved by collapsing the three-dimensional

flow undergoing the double homoclinic bifurcation to a two-dimensional branched template and using theory of knots and templates. This bifurcation scenario was named in [1] as the *period incrementing* scenario when analysing a piecewise-linear map using the offsets as parameters, because the periods of the periodic orbits emerging at the origin of the parameter space are incremented by a constant value. This is precisely what we prove independent of the particular topology in our work through the result shown in corollary 1. Additionally we make it independent of particular parametrizations in theorem 2. There we show for a general piecewise-smooth one-dimensional map that, whenever two (stable) fixed points simultaneously collide with the boundary in such a way that the signs of the associated eigenvalues are different, then a big bang bifurcation of the period incrementing type takes place.

Note that this scenario is also included in the gluing bifurcation considered in [7], as successive periodic orbits are created using always the same 'gluing orbit'. However, this leads to a much simpler bifurcation structure near the codimension-two bifurcation point than for the increasing–increasing case, in the sense the second scenario contents orbits that do not exist in the first one.

Although we assume in section 5 the existence of a period adding big bang bifurcation for the increasing–increasing case, we emphasize that a similar rigorous result for this case as the one presented here has not been stated (nor proved) anywhere.

Also in [11] one can find an accurate description of both scenarios together with the mechanisms that create the orbits. The objective there was to describe the bifurcation scenario for a homoclinic bifurcation of a flow with a single homoclinic orbit under the existence of what is called in [11] a *generalized homoclinic orbit*. This leads the first return map near the saddle point studied in [11] to be the one considered above, but with dependence only on a single parameter making these results valid only in a distance from the codimension-two bifurcation point. By understanding the flow as a small perturbation of one with two homoclinic orbits, it is argued in [11] that this also holds near the codimension-two bifurcation point. However, by embedding the period incrementing scenario in its natural two-dimensional parameter space, we show this independently of the flow stating it in the context of non-smooth dynamics. Moreover, we also show that the situation described there occurs for periodic orbits with arbitrarily large periods. In addition, this allows us to relax the global contracting condition required in [11] to be locally fulfilled.

This work is organized as follows. In section 2 we state some notation and definitions and present our result. In section 3 we prove this result for globally contracting maps for a concrete parametrization consisting on the offsets at the origin. After that, this result is extended in section 4.1 (corollary 1) to locally contracting ones near the boundary with the same parametrization. This can be proved directly but, for clarity, we prefer to do this intermediate step. In order to give details on how the bifurcations occur, we obtain in section 4.2 a first-order approximation of the border collision bifurcation curves that emerge at the big bang bifurcation for this concrete parametrization. Finally, we prove theorem 2 in section 4.3 and make the result independent of concrete parametrizations, permitting the parameters not only to vary the position of the fixed points but also the topology of the map. As these two sections are mainly technical, we encourage the reader not interested in the proofs to skip them up to section 5. There, by two examples, we verify the predictions. In addition, we also verify the increasing–increasing case, and conjecture that, in those examples, the period adding big bifurcation is caused by an infinite tree of big bang bifurcations of the period incrementing type. We finally conclude in section 6 with some remarks.

2. Definitions, properties and statement of the results

Before restricting ourselves to the class of maps we are interested in, let us start with some standard definitions and properties of the symbolic dynamics which we are going to use in this work.

Definition 1. *Given a map $f : \mathbb{R} \to \mathbb{R}$ and $x \in \mathbb{R}$, we define the symbolic representation of an orbit starting at x, also called the itinerary of x, as $I_f(x) \in \{\mathcal{L}, \mathcal{R}\}^{\mathbb{N}}$, where*

$$I_f(x)(i) = \begin{cases} \mathcal{L} & \text{if } f^i(x) \leqslant 0, \\ \mathcal{R} & \text{if } f^i(x) > 0. \end{cases} \qquad i \geqslant 0.$$

Definition 2. *If x belongs to a n-periodic orbit of a map f, then we will write $I_f(x) = \underline{\theta} := (\theta, \theta, \ldots)$ for some finite sequence θ of length n consisting of symbols $\mathcal{L}$ and $\mathcal{R}$.*

Definition 3. *Given the shift map σ defined as $\sigma(\alpha_1, \alpha_2, \alpha_3, \ldots) = (\alpha_2, \alpha_3, \ldots)$ where $\alpha_i \in \{\mathcal{L}, \mathcal{R}\}$, we will say that two n-periodic sequences, $\underline{\theta_1}$ and $\underline{\theta_2}$, are shift-equivalent (or just equivalent), $\underline{\theta_1} \sim \underline{\theta_2}$, if, and only if, there exists $0 \leqslant m < n$ such that $\sigma^m(\underline{\theta_1}) = \underline{\theta_2}$.*

It is easy to see that the relation $\sim$ defines an equivalence class in the set of symbolic sequences.

Definition 4. *We will say that a n-periodic orbit $x_1, \ldots, x_n$ of a map f is of type $\underline{\theta}$ if one has $I_f(x_i) \sim \underline{\theta}$, with $1 \leqslant i \leqslant n$ and θ a finite sequence of length n. We will also call it a θ-periodic orbit.*

Let us now consider a two-parametric map $f(x; c_\ell, c_r)$ of the form[5]

$$f(x; c_\ell, c_r) = \begin{cases} c_\ell + g_\ell(x; c_\ell, c_r) =: f_\ell(x; c_\ell, c_r) & \text{if } x \leqslant 0, \\ -c_r + g_r(x; c_\ell, c_r) =: f_r(x; c_\ell, c_r) & \text{if } x > 0, \end{cases} \tag{1}$$

such that

C.1 g_ℓ and g_r are $C^\infty(\mathbb{R})$ functions such that for $i, j \in \{\ell, r\}$

$$g_i(0; c_\ell, c_r) = 0$$

and the limit

$$\lim_{x \to 0} \frac{g_i(x; c_\ell, c_r)}{g_i(x; 0, 0)}$$

exists,

C.2 there exists $\varepsilon_\ell > 0$ such that $0 < g'_\ell(x; c_\ell, c_r) < 1$ $\forall x \in (-\varepsilon_\ell, 0)$ if $0 \leqslant c_\ell, c_r \ll 1$,

C.3 there exists $\varepsilon_r > 0$ such that $-1 < g'_r(x; c_\ell, c_r) < 0$ $\forall x \in (0, \varepsilon_r)$ if $0 \leqslant c_\ell, c_r \ll 1$,

where

$$g'(x; c_\ell, c_r) = \frac{\partial g(x; c_\ell, c_r)}{\partial x}.$$

Note that conditions C.2 and C.3 allow $g_i(x; c_\ell, c_r)$ to have zero slope at $x = 0$.

Note also that if $-1 \ll c_\ell, c_r < 0$ then the map has two fixed points, one at every side of $x = 0$ (see figure 1). Due to C.2 and C.3, both fixed points are attracting and, therefore, all orbits with sufficiently small initial conditions will be attracted to one of them, depending on the sign of the initial condition. If one of the parameters c_ℓ, c_r becomes positive, the corresponding fixed point disappears (becomes virtual through a border collision bifurcation) and all those orbits will be attracted to the other fixed point. However, if both parameters are

[5] We will also avoid writing the dependence on the parameters explicitly and we will refer to it just as $f(x)$ or f.

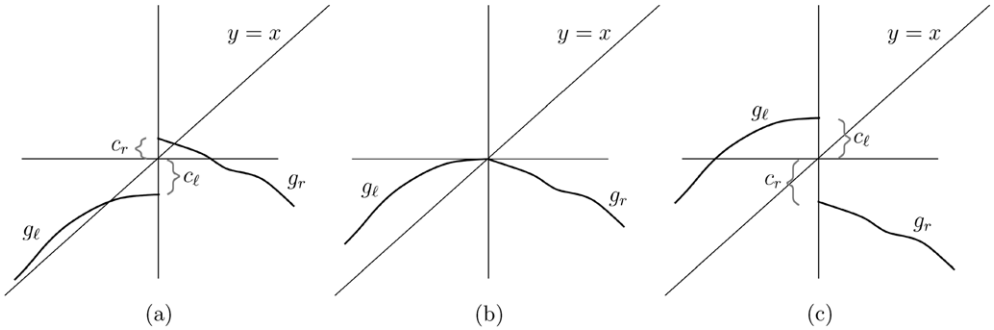

Figure 1. Influence of the parameters c_ℓ, c_r on a map as defined in (2). (*a*) $c_\ell, c_r < 0$, (*b*) $c_\ell = c_r = 0$ and (*c*) $c_\ell, c_r > 0$.

positive but small enough, both fixed points disappear (are virtual) and the orbits starting near the origin stay forever near the origin jumping from one side of $x = 0$ to the other one. The possible asymptotic behaviours of these orbits is precisely what our result describes, which is reflected in the next

Theorem 1. *Let f be a map of type (1) fulfilling conditions C.1–C.3. Then, there exists $\varepsilon_0 > 0$ such that, for every $n > 0$ and every $\varepsilon_0 > \varepsilon > 0$,*

- *(a) There exist two curves*[6] *in parameter space $c_\ell \times c_r$, $\xi^d_{\mathcal{RL}^{n-1}}(c_\ell)$ and $\xi^c_{\mathcal{RL}^{n+1}}(c_\ell)$, passing through the origin, such that for every $0 < c_\ell < \varepsilon$ with $\xi^d_{\mathcal{RL}^{n-1}}(c_\ell) < c_r < \xi^c_{\mathcal{RL}^{n+1}}(c_\ell)$, there exists a unique periodic orbit, which is stable and of type $\underline{\mathcal{RL}^n}$.*
- *(b) For every $0 < c_\ell < \varepsilon$, $\xi^c_{\mathcal{RL}^{n+1}}(c_\ell) < c_r < \xi^d_{\mathcal{RL}^n}(c_\ell)$, there coexist two periodic orbits, which are stable and of type $\underline{\mathcal{RL}^n}$ and $\underline{\mathcal{RL}^{n+1}}$.*

Moreover, for $(c_\ell, c_r) = (0, 0)$ there exists an open set containing the origin where the unique invariant object is the stable fixed point $x = 0$.

This means that, when considering the parameter space $c_\ell \times c_r \simeq \mathbb{R}^2$, there exists an infinite number of border collision bifurcation curves, $\xi^{d,c}_{\mathcal{RL}^n}$, emerging from the origin, separating all the possible dynamics that one can find near $x = 0$. These curves are ordered anti-clockwise as follows (see also figure 7(*b*) for a graphical explanation). Given $n \geqslant 1$, one first finds a curve where an $\underline{\mathcal{RL}^n}$-periodic orbit is created through a border collision, $\xi^c_{\mathcal{RL}^n}$, and coexists with another of type $\underline{\mathcal{RL}^{n-1}}$ until one finds the curve $\xi^d_{\mathcal{RL}^{n-1}}$ where the $\underline{\mathcal{RL}^{n-1}}$ orbit is destroyed. After that, only the $\underline{\mathcal{RL}^n}$-periodic orbit exists until the next border collision bifurcation occurs at the curve $\xi^c_{\mathcal{RL}^{n+1}}$ where a periodic orbit of type $\underline{\mathcal{RL}^{n+1}}$ is created. From there on, both orbits coexist until the $\underline{\mathcal{RL}^n}$-periodic orbit is destroyed at $\xi^d_{\mathcal{RL}^n}$. This is repeated for all n ad infinitum starting with the curve $\xi^c_{\mathcal{RL}}$, which is located in the 4th quadrant, and followed by the curve $\xi^d_{\mathcal{R}}$, which is the (positive) horizontal axis. Note that, following this point of view, the curve $\xi^c_{\mathcal{R}}$ is in fact the negative horizontal axis. All other border collision bifurcation curves mentioned above are located in the first quadrant and accumulate at the vertical axis. Details on how these bifurcation curves are obtained will be given in section 4.2 for the case that the functions g_ℓ and g_r do not depend on the parameters c_ℓ, c_r. As already stated in theorem 1, all the dynamics described above disappear exactly at the origin of the parameter space, where only a stable fixed point exists.

[6] The meaning of the upper indices d and c refer to 'creation' and 'destruction' of the corresponding periodic orbits. These terms of course depend on the point of view that one uses to observe the bifurcation scenario. We choose here to describe the bifurcation curves in the anti-clockwise order.

Obviously, if one interchanges ℓ by r in conditions C.2 and C.3 (decreasing–increasing case) and $\mathcal{L}$ by $\mathcal{R}$ everything above holds. That is, periodic orbits of type $\underline{\mathcal{RL}^n}$ become periodic orbits of type $\underline{\mathcal{LR}^n}$.

Regarding what has been said in the introduction, we will refer to the point $(c_\ell, c_r) = (0, 0)$ as a *big bang* bifurcation. In particular, for the situation described above one has the following

Definition 5. *Let B be a point in a two-dimensional parameter space such that the bifurcation scenario along the boundary of an arbitrary small neighbourhood of B is equivalent to the one described in theorem 1 for the origin. Then we will say that there exists a big bang bifurcation of period incrementing type in B.*

Then one can formulate theorem 1 in a more compact form as

Theorem 2. *For a map of type (1) which satisfies conditions C.1–C.3, the origin of the parameter space $c_r \times c_\ell$ represents a big bang bifurcation point of the period incrementing type.*

3. Increasing–decreasing globally contracting maps

As already mentioned in the introduction, in this section we will prove theorem 2 hardening conditions C.1–C.3. On the one hand, we will assume g_i to be globally contracting and not only near $x = 0$. In addition, we will omit the dependence of g_i on the parameters. Then, in section 4.1 using a simple result (lemma 8) we will see that theorem 2 also holds under these assumptions (corollary 1). Finally, using a perturbation argument, we will prove theorem 2 for conditions C.1–C.3.

Before going into details, let us state the strategy that we are going to follow. In order to show that only $\underline{\mathcal{RL}^n}$-periodic orbits are possible for $c_\ell, c_r > 0$, we will show that other type of periodic orbits cannot exist (lemmas 1, 2 and 3). This permits us, using the map $f_\ell^n(f_r)$, to show in lemma 6 that only a periodic orbit of type $\underline{\mathcal{RL}^n}$ can exist for some n. After that, considering the sequence of preimages of 0 under the action of f_ℓ, we will see that $\underline{\mathcal{RL}^n}$-periodic orbits exist for every n (lemma 7), that they are created and destroyed via border collision bifurcations and that at most two of them can coexist (lemma 5).

Let us consider a map as defined in (1) but relaxing the dependence on the parameters

$$f(x; c_\ell, c_r) = \begin{cases} c_\ell + g_\ell(x) =: f_\ell(x; c_\ell) & \text{if } x \leqslant 0, \\ -c_r + g_r(x) =: f_r(x; c_r) & \text{if } x > 0, \end{cases} \tag{2}$$

such that

C.1′ $g_\ell(x)$ and $g_r(x)$ are $C^\infty(\mathbb{R})$ functions such that $g_r(0) = g_\ell(0) = 0$
C.2′ $0 < g_\ell'(x) < 1$ if $x < 0$
C.3′ $-1 < g_r'(x) < 0$ if $x > 0$
C.4′ $\lim_{x\to\pm\infty} f(x; c_\ell, c_r) = -\infty$.

We start the proofs of these results with the following lemma.

Lemma 1. *Given $\theta = I_f(x)$ with f as defined in (2) fulfilling conditions C.1′–C.4′, if $I_f(x)(i) = \mathcal{R}$ and $c_r > 0$ then $I_f(x)(i + 1) = \mathcal{L}$. That is, no consecutive $\mathcal{R}$'s are possible in θ.*

Proof. Obvious, as $(0, \infty)$ is mapped into $(-\infty, 0)$. □

Remark 1. Note that the previous lemma does not need $I_f(x)$ to be a periodic sequence.

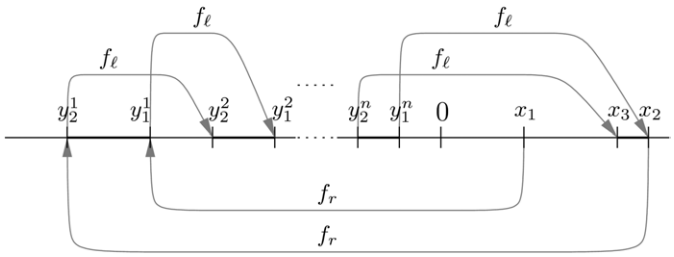

Figure 2. 'Trapped' orbit.

Lemma 1 obviously prohibits $\underline{\mathcal{R}^n}$-periodic orbits to exist. Although two consecutives $\mathcal{L}$'s are possible, $\underline{\mathcal{L}^n}$-periodic orbits are not, as the next result shows.

Lemma 2. *If x belongs to a periodic orbit of a map f as defined in (2) fulfilling conditions C.1′–C.4′, then, if $c_\ell > 0$ there exists an i such that $I_f(x)(i) = \mathcal{R}$.*

Proof. If $x > 0$, then one has $I_f(x)(0) = \mathcal{R}$. Otherwise, as f_ℓ is monotonically increasing with slope less than one and $f_\ell(0) > 0$, further iterates of x under the action of f_ℓ will necessarily reach the positive domain. □

As a next step we show now that the word $\mathcal{R}\mathcal{L}^n\mathcal{R}\mathcal{L}^n$ cannot be contained in any periodic orbit. It is worth emphasizing that with such a word, we obviously refer here (and in the following) to the compact representation, that is, it has to be followed by an $\mathcal{R}$, because a successive $\mathcal{L}$ would lead to the word $\mathcal{R}\mathcal{L}^n\mathcal{R}\mathcal{L}^{n+1}$. This result is shown in the next lemma based on a similar one presented in [10]. It is stated there, using geometrical arguments in the Lorenz template, that similar orbits are not possible for a three-dimensional flow undergoing a homoclinic bifurcation of the single twisted butterfly type. By contrast, we will use here only the nature of the map to prove it.

Lemma 3. *If f is of type (2) with $c_\ell, c_r > 0$, holding C.1′–C.4′, and there exists x_1 such that $I_f(x_1) = \underline{\theta}$, then the word $\mathcal{R}\mathcal{L}^n\mathcal{R}\mathcal{L}^n$ cannot be contained in θ.*

Proof. Let us suppose that there exists x_1 such that $I_f(x_1) = \underline{\theta}$ with $\theta = \mathcal{R}\mathcal{L}^n\mathcal{R}\mathcal{L}^n\theta_2$ for some finite word θ_2. Note that using the relation $\sim$ one can consider that θ is given in this form. Let us write this periodic orbit as

$$\underbrace{x_1, y_1^1, y_1^2, \ldots, y_1^n, x_2, y_2^1, y_2^2, \ldots, y_2^n}_{\mathcal{R}\mathcal{L}^n\mathcal{R}\mathcal{L}^n}, \underbrace{x_3, \ldots,}_{\theta_2} \underbrace{x_1, \ldots}_{\mathcal{R}\mathcal{L}^n\mathcal{R}\mathcal{L}^n}, \ldots,$$

where $x_i > 0$ and $y_i^j < 0$ (see figure 2). Let us also assume that $x_1 < x_2$ (otherwise the same argument can be performed with the points x_2 and x_3) and let us iterate the whole interval $[x_1, x_2]$. As f_r is decreasing and $c_r > 0$, $f_r([x_1, x_2]) = [y_2^1, y_1^1]$ with $f_r(x_2) = y_2^1 < f_r(x_1) = y_1^1 < 0$, the interval is twisted. Moreover, as f_r and f_ℓ are, respectively, decreasing and increasing contracting functions, we have

$$\mu([x_1, x_2]) > \mu([y_2^1, y_1^1]) > \mu([y_2^2, y_1^2]) > \cdots > \mu([y_2^n, y_1^n]) > \mu([x_3, x_2]),$$

where $\mu([a, b]) = |b - a|$ is the length of the interval $[a, b]$.

Now, as f_ℓ preserves orientation and the length of $[x_1, x_2]$ is decreased, $x_3 \in (x_1, x_2)$ and therefore $y_3^1 = f_r(x_3)$ needs also n iterations to return to the right side.

Repeating the same argument with $[x_3, x_2]$, one has that $f_l^n(y_3^1) = x_4 \in (x_3, x_2)$. Iterating the argument, the orbit of x_1 will be 'trapped' in (x_3, x_2) and will never reach x_1 again, so it cannot be periodic. □

Remark 2. Note that it is crucial in the last proof that both points x_1 and x_2 return to the right domain $(0, \infty)$ after exactly the same number n of iterations under the action of f_ℓ. That is, the interval $f^m([x_1, x_2])$ remains connected for all m.

Before considering periodic sequences containing the word $\mathcal{RL}^n\mathcal{RL}^m$ with $n \neq m$, let us state some properties and definitions of maps of type (2) fulfilling conditions C.1′–C.4′.

We first note that the left branch f_ℓ reaches its maximum value at $x = 0$ ($f_\ell(0) = c_\ell > 0$) and, therefore, when a point $y < 0$ is re-injected into the right domain by f_ℓ it has to be necessarily in $(0, c_\ell]$. On the other hand, as f_r is monotonically decreasing, every point $x \in (0, c_\ell]$ will be injected into the left domain in the interval $[\nu, 0]$, where $\nu = f_r(c_\ell) < 0$. Hence, the interval $[\nu, c_\ell]$ acts as an 'absorbing' interval as all orbits starting at any point $x \in \mathbb{R}$ will reach it after some number of iterations and will never leave it. Therefore we have the following lemma.

Lemma 4. *Let $f(x)$ be a map of type (2) which fulfils conditions C.1′–C.4′ and let $\nu = f_r(c_\ell)$. For every $x \in \mathbb{R}$ there exists an m_0 such that $f^m(x) \in [\nu, c_\ell]$ $\forall m \geqslant m_0$. Therefore, the map f can be considered as a map on the interval $[\nu, c_\ell]$:*

$$f : [\nu, c_\ell] \to [\nu, c_\ell]$$

Remark 3. Note that this global reduction is true as the functions g_ℓ/g_r are globally increasing/decreasing and contractive (C.1′–C.4′). In the next section, where conditions C.1′–C.4′ are going to be relaxed, this reduction will be valid only locally.

Let us now consider the sequences $\{a_n\}$ and $\{b_n\}$ formed, respectively, by the preimages of 0 by the left branch and by the preimages of these preimages by the right branch

$$a_0 = 0, \quad a_n = f_\ell^{-1}(a_{n-1}) \qquad \text{with } n > 0, \tag{3}$$

$$b_n = f_r^{-1}(a_n) \qquad \text{with } n \geqslant n_0, \tag{4}$$

with some n_0 as explained below (see figure 3). Note that, as f_ℓ is a monotonically increasing function, if $c_\ell > 0$ the sequence $\{a_n\}$ verifies $a_{n+1} < a_n \leqslant 0$ $\forall n \geqslant 0$.[7] Although the preimages of 0 by the left branch (a_n) exist $\forall n$, b_n is defined for $n \geqslant n_0$ where n_0 is such that $a_{n_0} \leqslant -c_r < a_{n_0-1}$.

Due to the contractiveness of both functions f_ℓ and f_r, the following inequalities hold

$$\frac{\mu([a_{n+1}, a_n])}{\mu([a_n, a_{n-1}])} > 1, \qquad n > 0, \tag{5}$$

$$\frac{\mu([b_n, b_{n+1}])}{\mu([b_{n-1}, b_n])} > 1, \qquad n > n_0.$$

The sequence $\{a_n\}$ defined in equation (3) splits the interval $(-\infty, 0]$ into sub-intervals of the form $(a_{n+1}, a_n]$ (see figure 3) such that $\forall y \in (a_{n+1}, a_n]$ the number of iterations needed for y to return to the right domain is exactly $n + 1$. On the other hand, the intervals $(0, b_{n_0})$ and $[b_n, b_{n+1})$ with $n \geqslant n_0$, form a partition of $(0, \infty)$, such that $\forall x \in [b_n, b_{n+1})$ the point $f_r(x)$ needs exactly $n + 1$ iterations by f_ℓ to return to the positive domain.

For a fixed value $(c_\ell, c_r) \in \mathbb{R}^+ \times \mathbb{R}^+$, the number of iterations that a periodic orbit can perform in the negative domain is determined by the number of elements of the sequence $\{b_n\}$

[7] Note that $f^0(0) = 0$ as the function $f^0(x)$ is the identity.

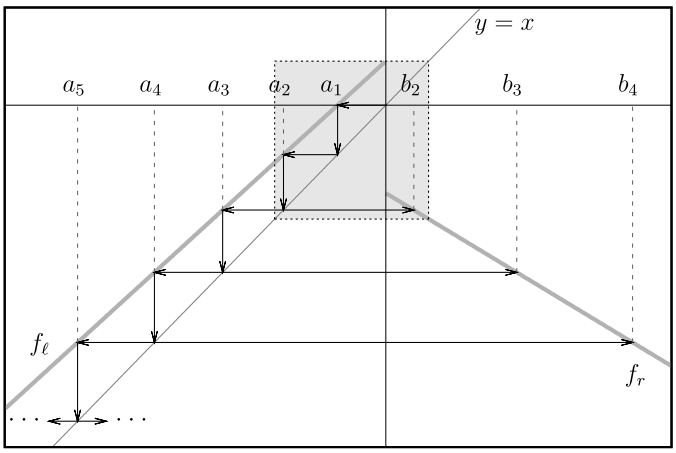

Figure 3. Definition of the sequences $\{a_n\}$ and $\{b_n\}$. The dotted box corresponds to the absorbing interval.

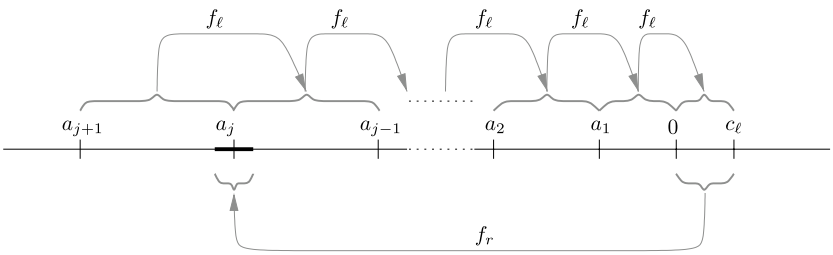

Figure 4. Backward and forward iterates of $(0, c_\ell]$. $f_r((0, c_\ell])$ (dark segment) is smaller than $f_\ell^{-n}((0, c_\ell])$ $\forall n$. Therefore, at most one a_j can be reached by $f_r((0, c_\ell])$.

contained in the absorbing interval $[\nu, c_\ell]$. For example if b_2 and b_3 would be contained in the absorbing interval $[\nu, c_l]$, then the number of iterations of a periodic orbit can be two, three or four. However, as the next result shows, at most one element of the sequence $\{b_n\}$ can be contained in the absorbing interval $[\nu, c_\ell]$.

Lemma 5. *If f is a map of type (2) fulfilling conditions C.1′–C.4′, then there exists at most one a_j (equiv. b_j) such that $a_j \in f_r((0, c_\ell])$ (equiv. $b_j \in (0, c_\ell]$).*

Proof. Recalling that $c_\ell = f_\ell(0)$, one has (see figure 4)

$$[a_{n+1}, a_n] = f_\ell^{-1}([a_n, a_{n-1}]),$$
$$[a_1, 0] = f_\ell^{-1}([0, c_\ell]).$$

Using the property shown in equation (5) one has

$$\mu([0, c_\ell]) < \mu([a_{n+1}, a_n]) \qquad \forall n,$$

and since f_r is a contractive function one obtains

$$\mu(f_r((0, c_\ell]) < \mu([a_{n+1}, a_n]) \qquad \forall n.$$

Therefore, at most one a_n can be located in $f((0, c_\ell])$. □

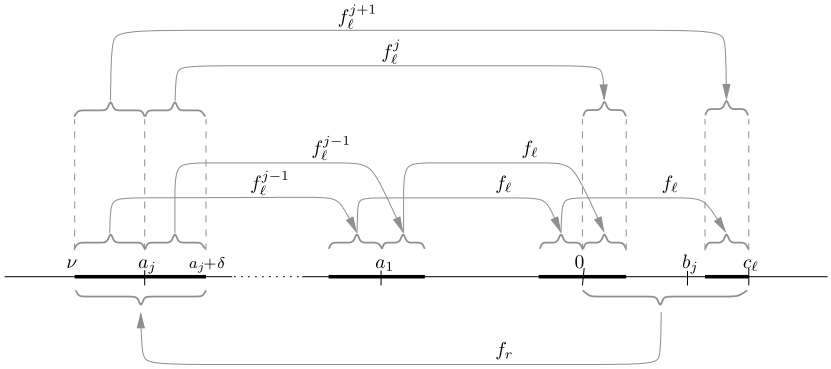

Figure 5. The interval $f_r((0, c_\ell])$ is split when it returns to the right domain.

For a fixed j, the uniqueness of such a b_j (in the case of existence) in the last lemma implies that the periodic sequences of a map under the considered conditions can be either $\underline{\mathcal{RL}^j}$, $\underline{\mathcal{RL}^{j+1}}$ or sequences containing these two words only. However, what we want to show is that the last case is not possible and in fact the only admissible periodic sequences are exactly $\underline{\mathcal{RL}^j}$ and $\underline{\mathcal{RL}^{j+1}}$. Therefore, let us consider the two only possible cases: for a certain j, either $(0, c_\ell] \subset (b_j, b_{j+1})$ (which means $b_j = 0$ or $b_j \notin [0, c_\ell]$) or $(0, c_\ell] = (0, b_j) \cup [b_j, c_\ell]$ (which means $b_j \in (0, c_\ell]$) ($c_\ell < b_{j+1}$), which is the case shown in figure 3.

In the first case, as the periodic orbits have to be contained in the interval $[\nu, c_\ell]$, they always need the same number of iterations on the negative domain and the result comes from lemmas 1, 2 and 3.

In the second case, we have to show that if a periodic orbit reaches $(0, b_j)$ it cannot reach $[b_j, c_\ell]$ and vice versa, that is, once an orbit enters the absorbing interval $[\nu, c_\ell]$, the number of iterations needed to return to the positive domain is preserved and is either j or $j + 1$. Both cases are included in the following lemma.

Lemma 6. *Let f be a map as defined in (2) fulfilling conditions C.1′–C.4′. If $x \in \mathbb{R}$ belongs to a periodic orbit of f then there exists $n > 0$ such that $I_f(x) = \underline{\mathcal{RL}^n}$ up to shift-equivalence.*

Proof. If $\nexists\, a_j \in f_r((0, c_\ell])$, then $f_r((0, c_\ell]) \subset (a_n, a_{n-1})$ for some n and

$$f_\ell^n(f_r\,(0, c_\ell])) \subset (0, c_\ell].$$

Due to the contractiveness, the map $f_\ell^n f_r(x)$ has a fixed point and f an $\underline{\mathcal{L}^n\mathcal{R}}$-periodic orbit. By lemmas 1, 2 and 3, it is the unique one.

Now let us suppose that there exists $a_j \in f_r((0, c_\ell])$ which, by lemma 5, must be unique. We also have a unique $b_j \in (0, c_\ell]$. As f_r is monotonically decreasing and thus the interval $(0, c_\ell]$ is inverted, we can write

$$f_r((0, c_\ell]) = [\nu, a_j + \delta)$$

for some $\delta > 0$.

As f_ℓ is continuous in $(-\infty, 0]$ and $f_\ell(a_n) = a_{n-1}$ $\forall n > 1$, the interval $f_\ell^n([\nu, a_j + \delta))$ remains connected and contains a_{j-n} for $n = 1, \ldots, j$ (see figure 5). For $n = j$, the interval contains 0 and therefore it contains positive and negative points. The positive ones are immediately mapped into $(a_j, a_j + \delta)$ by f_r in such a way that $f_r(0^+) = (a_j + \delta)^-$. Negative points need one more iteration by f_ℓ and will be mapped into $(b_j, c_\ell]$ with $f_\ell(0^-) = c_\ell^-$, so

the initial interval is split. After that, these points will be mapped into $[v, a_j)$ verifying that $f_r(c_\ell^-) = v^+$. Summarizing,

$$f_r((0, b_j)) = (a_j, a_j + \delta),$$
$$f_r([b_j, c_\ell] = [v, a_j]$$

and

$$f_\ell^{j+1}([v, a_j]) \subset [b_j, c_\ell],$$
$$f_\ell^{j}((a_j, a_j + \delta)) \subset (0, b_j),$$

so

$$f_\ell^{j+1}(f_r([b_j, c_\ell])) \subset [b_j, c_\ell],$$
$$f_\ell^{j}(f_r(0, b_j)) \subset (0, b_j),$$

and, for an orbit starting in $(0, c_\ell]$, the number of steps performed in the negative domain before being re-injected to the positive domain will remain constant and equal to j or $j+1$ depending on whether it starts in $(0, b_j)$ or $[b_j, c_\ell]$, respectively. Therefore, only symbolic sequences of the form $\mathcal{RL}^j\mathcal{RL}^j\ldots$ or $\mathcal{RL}^{j+1}\mathcal{RL}^{j+1}\ldots$ with starting points in $(0, c_\ell]$ are possible.

As has been proven above, that the number of steps on the left side of a periodic orbit must be preserved, we can apply lemma 3 to show that if x belongs to a periodic orbit of a map under the considered conditions, then necessarily $I_f(x) = \underline{\mathcal{RL}^n}$ for some $n > 0$. □

Now we ask about the reciprocal of lemma 6, that is, we want to show that periodic orbits of type $\underline{\mathcal{RL}^n}$ exist $\forall n > 0$.

Lemma 7. *Let f be of the form defined in (2) and fulfilling conditions C.1′–C.4′. Then, for every $n \geqslant 1$ and every $c_\ell > 0$, there exists $c_r > 0$ such that f possesses an orbit with the symbolic sequence $\underline{\mathcal{RL}^n}$.*

The proof of this lemma is in fact an extension of the arguments presented in [11] section 3.3.

Proof. It is clear that for every $n \geqslant 2$ and every $c_\ell > 0$ there exists $c_r > 0$ such that

$$f_r((0, c_\ell]) \cap [a_n, a_{n-1}] \neq \emptyset,$$

which can be given due to one of the next three situations (see figures 4 and 5)

S.1 $a_{n-1} \in f_r((0, c_\ell])$
S.2 $f_r((0, c_\ell]) \subset (a_n, a_{n-1})$
S.3 $a_n \in f_r((0, c_\ell])$

If S.1 holds, $b_{n-1} \in (0, c_\ell]$ and

$$f_\ell^n f_r : [b_{n-1}, c_\ell] \longrightarrow [b_{n-1}, c_\ell],$$
$$f_\ell^{n-1} f_r : (0, b_{n-1}) \longrightarrow (0, b_{n-1}),$$

are continuous contracting functions which must have a unique (stable) fixed point. Therefore, two stable periodic orbits $\underline{\mathcal{RL}^n}$ and $\underline{\mathcal{RL}^{n-1}}$ coexist. Note that for $n = 2$ this proves also the existence of a $\underline{\mathcal{RL}}$ orbit.

In the second case (S.2), $b_{n-1} \notin (0, c_\ell]$ ($[0, c_\ell] \subset (b_{n-1}, b_n)$) and

$$f_\ell^n f_r : (0, c_\ell] \longrightarrow (0, c_\ell]$$

is a continuous contracting function which also must have a unique (stable) fixed point. In this case, there exists a unique periodic orbit of type $\underline{\mathcal{RL}^n}$ which is the unique attractor in $(0, c_\ell]$.

Finally, if S.3 holds, replacing n by $n - 1$ and arguing as in S.1, one has that a stable periodic orbit of type $\underline{\mathcal{RL}^n}$ coexists with a stable $\underline{\mathcal{RL}^{n+1}}$-periodic one. □

Remark 4. By contrast to all orbits $\underline{\mathcal{RL}^n}$ with $n \geqslant 2$, the periodic orbit $\underline{\mathcal{RL}}$ exists not only for $c_r > 0$ but also for $c_r \leqslant 0$. In that case, it coexists with the fixed point $\underline{\mathcal{R}}$ ($\underline{\mathcal{L}^0\mathcal{R}}$).

Remark 5. Note that the transitions between cases S.1, S.2 and S.3 are given by border collision bifurcations where the respective periodic orbits are created or destroyed when they collide with the boundary $x = 0$. This defines the curves ξ^c and ξ^d used in theorem 1. See section 4.2 for more details.

Remark 6. As is known, invariant objects of piecewise-smooth systems do not necessarily have to be separated by another invariant object. In this case, the coexistence of stable periodic objects may also be separated by the discontinuity (and its preimages) (see [24] for an extensive overview about piecewise-smooth dynamics).

Theorem 3. *For a map of type (2) which fulfils conditions C.1′–C.4′, the origin of the parameter space $c_\ell \times c_r$ represents a big bang bifurcation point of the period incrementing type.*

Proof. It is clear that for $(c_\ell, c_r) = (0, 0)$ the map f possesses a stable fixed point at $x = 0$. In a first step we have to show that an infinite number of bifurcation curves separating existence regions of different periodic orbits are issuing from the origin. In a second step we have to show that a smooth change in the parameters across the bifurcation curve confining the regions of existence of a unique $\underline{\mathcal{RL}^n}$ orbit lead to the creation of (coexisting) $\underline{\mathcal{RL}^{n+1}}$- or $\underline{\mathcal{RL}^{n-1}}$-periodic orbits.

The key to show the first step is the fact that the sequence $\{a_n\}$ collapses to the origin as $c_\ell \to 0$, that is

$$\lim_{c_\ell \to 0} a_n = 0 \qquad \forall n \geqslant 1.$$

This is due to the continuity of f_ℓ and the fact that it is a monotonically increasing function. As $[a_1, 0] = f_\ell^{-1}([0, c_\ell])$ (compare figure 4), it is clear that $a_1 \to 0$ as $c_\ell \to 0$. Now, iterating the argument and using that $a_n = f_\ell^{-1}(a_{n-1})$, it is clear that for every $\varepsilon > 0$, arbitrarily small, there exists $c_\ell(\varepsilon)$ small enough such that $-\varepsilon < a_n < 0$. By lemma 7, there exists c_r such that $f_r((0, c_\ell])$ contains a_n and, therefore, a periodic orbit of type $\underline{\mathcal{RL}^n}$ exists.

On the other hand, it is clear that $c_r \to 0$ as $a_n \to 0$ and, therefore, a $\underline{\mathcal{RL}^n}$-periodic orbit exists for every n for values of (c_ℓ, c_r) arbitrarily close to the origin. Finally, if $(c_\ell, c_r) = (0, 0)$, the map possesses a stable fixed point which absorbs all orbits and thus all periodic orbits disappear at that point. □

4. Extension of the result

4.1. Increasing–decreasing locally contracting maps

In this section we relax the global monotonically contracting conditions C.1′–C.4′ to be fulfilled near the origin and show that the results of the previous section are valid sufficiently close to the origin of the parameter space. Thus, we restrict ourselves to maps of type (2) fulfilling

C.1″ g_ℓ and g_r are $C^\infty(\mathbb{R})$ functions such that $g_\ell(0) = g_r(0) = 0$
C.2″ There exists $\varepsilon_\ell > 0$ such that $0 < g'_\ell(x) < 1$ $\forall x \in (-\varepsilon_\ell, 0)$
C.3″ There exists $\varepsilon_r > 0$ such that $-1 < g'_r(x) < 0$ $\forall x \in (0, \varepsilon_r)$.

Due to the smoothness of functions f_ℓ and f_r near the origin, there exists an open neighbourhood of this point where both functions are contracting and which contains the absorbing interval $[\nu, c_\ell]$ if c_r and c_ℓ are small enough.

On the other hand, the values of c_r given by lemma 7 tend to 0 as $c_\ell \to 0^+$, and therefore all results of the previous section hold under these conditions.

From the previous arguments one has the next result.

Lemma 8. *Let f be a map of type (2) keeping conditions C.1″–C.3″. Then there exist c_ℓ^0 and c_r^0 such that if $0 < c_\ell < c_\ell^0$ and $0 < c_r < c_r^0$ f is contracting in $[v, c_\ell]$. Moreover, for every $c_r < c_r^0$ and every n, there exists $0 < \varepsilon < c_\ell^0$ such that $a_j \in [v, 0]$ $\forall j \leqslant n$ if $c_\ell < \varepsilon$.*

Corollary 1. *Under conditions C.1″–C.3″, a map of type (2) undergoes a big bang bifurcation of the period incrementing type at the origin of the parameter space $c_\ell \times c_r$.*

Remark 7. If one changes condition C.3′ by g_r to be a constant function for $x \geqslant 0$, then all the results presented above are still valid except for one detail. In such a case, one has only to take into account that, as $f_r((0, c_\ell])$ would be a single point. Then, conditions S.1 and S.3 in the proof of lemma 7 become $a_{n-1} = f_r((0, c_\ell])$ and $a_n = f_r((0, c_\ell])$, respectively, preventing the coexistence between two different orbits. Therefore, (b) in theorem 1 no longer holds as $\xi^c_{\mathcal{RL}^{n-1}} = \xi^d_{\mathcal{RL}^n}$. Such a situation has been referred to in the literature [1] as the *pure period incrementing* scenario, and therefore the origin of the parameter space represents a *pure period incrementing* big bang bifurcation.

Recalling remark 5, the orbits given in theorem 2 are created and destroyed at border collision bifurcations curves, which are mentioned in the first version of the same result, theorem 1. In the next section, approximating them up to first order, we will give details on how they are obtained.

4.2. Border collision curves near the origin

Given $n > 0$ and $c_\ell > 0$ (which we will always assume to be small enough), we know (lemma 7) that there exists $c_r > 0$ such that one of the next cases hold

S.1 $a_{n-1} \in f_r((0, c_\ell])$
S.2 $f_r((0, c_\ell]) \subset (a_n, a_{n-1})$
S.3 $a_n \in f_r((0, c_\ell])$

implying the existence of a $\underline{\mathcal{RL}^n}$-periodic orbit. As has been shown in the proof of lemma 7, every case above leads to different dynamics. Therefore, the limiting parameter values define a (border collision) bifurcation. Then for each of the cases above, for every c_ℓ we will find the extremal value of c_r and obtain the bifurcation curves, $\xi^{c,d}_{\mathcal{RL}^n}$ at which an $\underline{\mathcal{RL}^n}$ orbit is created or destroyed.

The smallest value of c_r which leads S.1 to be fulfilled is given by

$$f_r(c_\ell) = a_{n-1} \tag{6}$$

and corresponds to the creation of the periodic orbit $\underline{\mathcal{RL}^n}$ coexisting with the periodic orbit $\underline{\mathcal{RL}^{n-1}}$. The transition between S.1 and S.2 is given by

$$f_r(0) = a_{n-1},$$

where the periodic orbit $\underline{\mathcal{RL}^{n-1}}$ is destroyed leading the periodic orbit $\underline{\mathcal{RL}^n}$ to be the unique attractor (near the origin).

Increasing c_r, one finds the value of this parameter which satisfies the condition

$$f_r(c_\ell) = a_n.$$

At this parameter value, representing the transition from S.2 to S.3, the periodic orbit $\underline{\mathcal{RL}^{n+1}}$ is created and coexists with $\underline{\mathcal{RL}^n}$.

Finally, the next bifurcation is given by

$$f_r(0) = a_n \tag{7}$$

where the periodic orbit $\underline{\mathcal{RL}^n}$ is destroyed as S.3 no longer holds.
Summarizing, for every $c_\ell > 0$ and $n > 0$, equations (6) and (7) give the value of c_r for the border collision bifurcations where, respectively, the $\underline{\mathcal{RL}^n}$-periodic orbit is created and destroyed. Therefore, in parameter space, the respective border collision bifurcation curves in a sufficiently small open set $\mathcal{U}$ of the origin will be given by

$$\xi^c_{\mathcal{RL}^n} = \{(c_\ell, c_r) \in \mathcal{U},\ c_\ell > 0 \mid f_r(c_\ell) = a_{n-1}\},$$
$$\xi^d_{\mathcal{RL}^n} = \{(c_\ell, c_r) \in \mathcal{U},\ c_\ell > 0 \mid f_r(0) = a_n\}.$$

However, in order to obtain first-order approximation of these curves, it is more convenient to consider the equations

$$F^c(c_\ell, c_r) := f_\ell^{n-1}(f_r(c_\ell)) = 0, \tag{8}$$
$$F^d(c_\ell, c_r) := f_\ell^n f_r(0) = 0, \tag{9}$$

which are equivalent to (6) and (7), respectively. In addition, as

$$\frac{\partial F^c}{\partial c_r}(0,0) = \begin{cases} -1 & \text{if } n = 1, \\ -g'_\ell(0)^{n-1} & \text{if } n > 1, \end{cases}$$
$$\frac{\partial F^d}{\partial c_r}(0,0) = -g'_\ell(0)^n,$$

one can always write c_r as a function of c_ℓ if $g'_\ell(0) \neq 0$. Therefore, using

$$\frac{\partial F^c}{\partial c_\ell}(0,0) = \begin{cases} g'_r(0) & \text{if } n = 1, \\ 1 + g'_\ell(0) + g'_\ell(0)^2 & \\ \quad + \cdots + g'_\ell(0)^{n-1} g'_r(0) & \text{if } n > 1, \end{cases} \tag{10}$$

$$\frac{\partial F^d}{\partial c_\ell}(0,0) = 1 + g'_\ell(0) + g'_\ell(0)^2 + \cdots + g'_\ell(0)^{n-1} + g'_\ell(0)^n > 0 \tag{11}$$

and applying the implicit function theorem, the first-order approximation of the bifurcation curves is given by the expressions

$$c_r = \xi^c_{\mathcal{RL}^n}(c_\ell) = -\frac{\frac{\partial F^c}{\partial c_\ell}}{\frac{\partial F^c}{\partial c_r}} c_\ell + O(c_\ell^2)$$
$$= \frac{1 + g'_\ell(0) + g'_\ell(0)^2 + \cdots + g'_\ell(0)^{n-1} g'_r(0)}{g'_\ell(0)^{n-1}} c_\ell + O(c_\ell^2), \tag{12}$$

$$c_r = \xi^d_{\mathcal{RL}^n}(c_\ell) = -\frac{\frac{\partial F^d}{\partial c_\ell}}{\frac{\partial F^d}{\partial c_r}} c_\ell + O(c_\ell^2)$$
$$= \frac{1 + g'_\ell(0) + g'_\ell(0)^2 + \cdots + g'_\ell(0)^{n-1} + g'_\ell(0)^n}{g'_\ell(0)^n} c_\ell + O(c_\ell^2). \tag{13}$$

Remark 8. In the case that $g'_\ell(0) = 0$, all the bifurcation curves $\xi^{c,d}_{\mathcal{RL}^n}$, with $n > 1$, are vertical at the origin and one cannot proceed with this approach to obtain approximated expressions. However, one can always obtain c_ℓ as a function of c_r instead, although, in order to distinguish between the curves, a higher order analysis becomes necessary because all first-order approximations lead to the vertical axis.

Remark 9. Recalling that $f_\ell^0 = Id$, for $n = 1$ one has that

$$\frac{\partial F^c}{\partial c_\ell}(0,0) = g_r'(0),$$
$$\frac{\partial F^c}{\partial c_r}(0,0) = -1.$$

Hence, curve (12) becomes

$$\xi^c_{\mathcal{RL}}(c_\ell) = g_r'(0)c_\ell + O(c_\ell^2),$$

which, assuming $g_r'(0) \neq 0$, has negative slope. Thus, as mentioned in the discussion below theorem 1, this bifurcation curve is located in the fourth quadrant.

Using $n = 0$ in equation (9), it clearly comes that the curve $\xi^d_{\mathcal{R}}$ is the horizontal axis, $c_r = 0$.

As one can see from equations (12)–(13), all other bifurcation curves have positive slope and, hence, are located in the first quadrant.

4.3. Proof of theorem 2

In order to prove theorem 2 we first consider a map of the form (1) and obtain from it a new map

$$\tilde{f}(x) = \begin{cases} c_\ell + g_\ell(x;0,0) =: \tilde{f}_\ell(x;c_\ell) & x < 0, \\ -c_r + g_r(x;0,0) =: \tilde{f}_r(x;c_r) & x > 0, \end{cases} \tag{14}$$

which is of type (2) and fulfils conditions C.1″–C.3″. Note in particular that conditions C.2 and C.3 for a map of type (1) imply that (14) fulfils conditions C.2″ and C.3″. Therefore, corollary 1 applies and system (14) undergoes a big bang bifurcation of the period incrementing type at the origin of the parameter space $c_\ell \times c_r$. Then, one only needs to show that all the bifurcation curves issuing from the origin of the parameter space also exist for system (1). For that purpose, let us consider for example the bifurcation curve defined by the equation

$$\tilde{f}_\ell^n(\tilde{f}_r(0;c_r);c_\ell) = 0, \tag{15}$$

which, for convenience, we solve isolating c_ℓ as a function of c_r. Thus, recalling remarks 8 and 9, we know that (15) possesses a (unique) solution c_ℓ^* for every c_r arbitrarily small and for every $n \geqslant 1$, defining the border collision bifurcation curve $c_\ell = \tilde{\xi}^d_{\mathcal{RL}^n}(c_r)$. Now, we wonder whether the corresponding equation

$$f_\ell^n(f_r(0;c_\ell,c_r);c_\ell,c_r) = 0 \tag{16}$$

that defines the corresponding bifurcation curve for the original system can also be solved for c_ℓ for every c_r small. Note that the functions f_ℓ and f_r can be written as

$$f_\ell(x;c_\ell,c_r) = \tilde{f}_\ell(x;c_\ell) + G_\ell(x;c_\ell,c_r),$$
$$f_r(x;c_\ell,c_r) = \tilde{f}_r(x;c_r) + G_r(x;c_\ell,c_r),$$

with $G_i(x;0,0) = 0$ and $\frac{\partial G_i}{\partial j}(0;0,0) = 0$, $i \in \{\ell, r\}$ $j \in \{x, c_\ell, c_r\}$. As a consequence of that, a straight forward calculation shows that equation (16) can be written as

$$F(c_\ell,c_r) := f_\ell^n(f_r(0;c_\ell,c_r);c_\ell,c_r) = \tilde{f}_\ell^n(\tilde{f}_r(0;c_r);c_\ell) + G(c_\ell,c_r) = 0$$

with G containing only higher order terms, that is, $G(0,0) = 0$ and $\frac{\partial G}{\partial c_i}(0,0) = 0$ $i \in \{\ell, r\}$. Now, as

$$F(0,0) = 0, \qquad \frac{\partial F}{\partial c_\ell}(0,0) \neq 0,$$

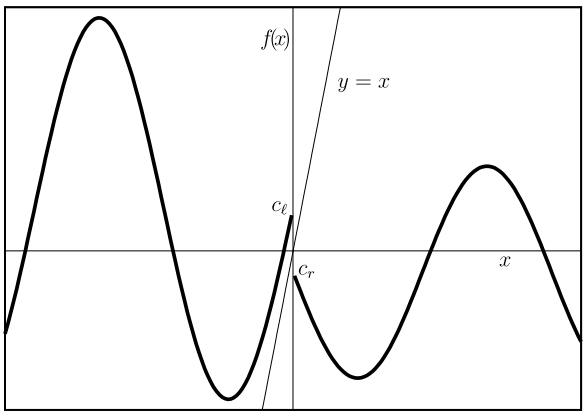

Figure 6. System function of example 1 defined in equation (18).

one can apply the implicit function theorem at $(c_\ell, c_r) = (0, 0)$ and show that equation (16) can be solved for c_ℓ. In addition, the fact that the limit

$$\lim_{x\to 0} \frac{g_\ell(x; c_\ell, c_r)}{g_\ell(x; 0, 0)}$$

exists, ensures that this solution will be of the form

$$c_\ell = \xi^d_{\mathcal{RL}^n}(c_r) = \tilde{\xi}^d_{\mathcal{RL}^n}(c_r) + \Psi(c_r), \tag{17}$$

where $\Psi(c_r)$ is such that

$$\lim_{c_r\to 0} \frac{\Psi(c_r)}{\tilde{\xi}^d_{\mathcal{RL}^n}(c_r)} = 0,$$

that is, $\Psi(c_r)$ depends on c_r in higher order terms than $\tilde{\xi}^d_{\mathcal{RL}^n}(c_r)$ does. Therefore, by considering c_r small enough, it is clear that both bifurcation curves are arbitrarily close to each other.

Finally, arguing similarly with the other bifurcation curves, it comes that the bifurcation scenarios of systems (1) and (2) near $(c_\ell, c_r) = (0, 0)$ are the same, which proves the result.

5. Examples

In this section we will illustrate the results obtained so far with two examples.

5.1. Example 1

Let us consider

$$f(x) = \begin{cases} c_\ell + \frac{9}{10}\sin(x) =: f_\ell(x) & \text{if } x \leqslant 0, \\ -c_r - \frac{1}{2}\sin(x) =: f_r(x) & \text{if } x > 0 \end{cases} \tag{18}$$

shown in figure 6, which fulfils conditions C.1″–C.3″ and, in particular, C.1–C.3.

As one can see in figure 7, there exists a big bang bifurcation of the period incrementing type at the origin of the parameter space $c_\ell \times c_r$, as predicted by theorem 2 or corollary 1, which also applies. A global overview of the bifurcation scenario is presented in figure 7(*a*), and a magnification near the origin of this space is shown in figure 7(*b*). There one can observe the expected infinite number of border collision bifurcation curves separating the regions of existence of the different periodic orbits. There it is also shown the first-order approximation

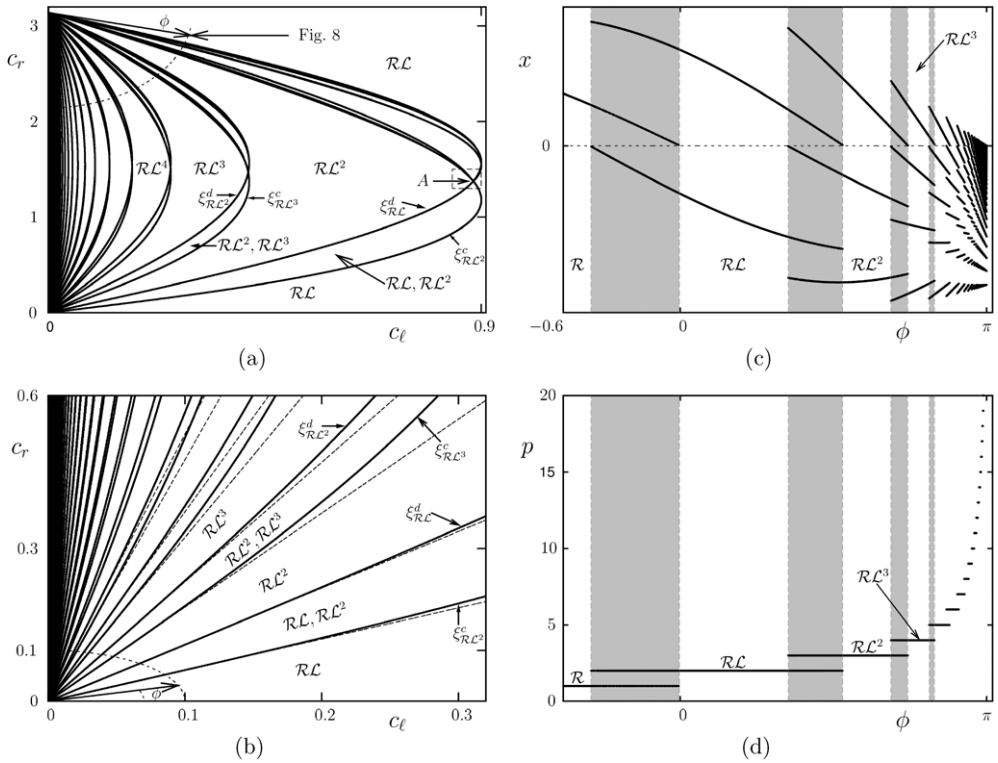

Figure 7. (*a*) Border collision bifurcation curves for example 1. A blow up of the neighbourhood of the point A is shown in figure 9(*a*). (*b*) Numerical (black) and first-order approximations of the analytical (grey) border collision bifurcation curves near the origin. (*c*) Bifurcation diagram through the curve surrounding the origin in (*b*) parametrized by ϕ anti-clockwise. The grey regions indicate coexistence between two periodic orbits (*d*) periods of the detected orbits in (*c*).

of the bifurcation curves reported in section 4.2. As one can see in the one-dimensional bifurcation diagram presented in figure 7(*c*) along the curve parametrized by ϕ in figure 7(*b*), the periodic orbits that exist near the origin are of type $\underline{\mathcal{RL}^n}$. As labelled in the figures, there exist regions where only one periodic orbit of type $\underline{\mathcal{RL}^n}$ exists, and there exist other regions where two periodic orbits of type $\underline{\mathcal{RL}^n}$ and $\underline{\mathcal{RL}^{n+1}}$ coexist.

As one can see in figure 7(*a*), near $(0, \pi)$ there exists another point where an infinite number of bifurcation curves seem to emerge from.

In order to investigate this point in more detail and see whether the result presented above can be applied, let us first note that it is given by the intersection between the border collision bifurcation curves $\xi^d_{\mathcal{R}}$ (the vertical axis) and $\xi^d_{\mathcal{RL}}$. This means that, at this point, a periodic orbit of type $\underline{\mathcal{RL}}$ collides with the boundary together with the fixed point $\underline{\mathcal{L}}$. This is exactly what we have considered in this work, the simultaneous collision of two fixed points with the boundary. Let us therefore consider the following composite map

$$f_2(x) = \begin{cases} f_\ell(x) & \text{if } x \leqslant 0, \\ f_\ell f_r(x) & \text{if } x > 0, \end{cases} \tag{19}$$

which collapses the $\underline{\mathcal{RL}}$-periodic orbit of (18) to the fixed point $\underline{\mathcal{R}}$ of (19). Easily, one sees that, for $(c_\ell, c_r) = (0^+, \pi^-)$, $f_\ell(0) = 0^+$, $f_\ell f_r(0) = 0^-$, $f'_\ell(0^-) = \frac{9}{10}$ and $(f_\ell f_r)'(0^+) = \frac{9}{20}$. This means that $f_2(x)$ possesses two stable fixed points which, when increasing c_ℓ and decreasing

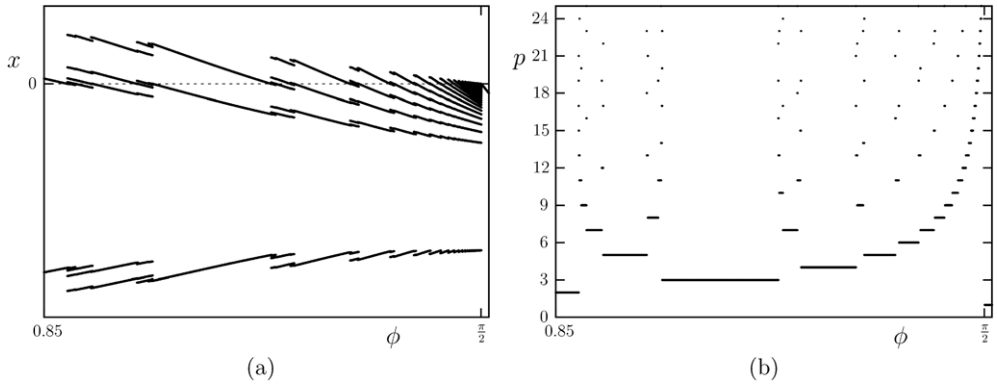

Figure 8. Bifurcation structure around the period adding big bang bifurcation occurring at $(0, \pi)$ for example 1. (*a*) Bifurcation diagram along the curve labelled in figure 7(*a*) and parametrized clockwise by ϕ . (*b*) Periods of the detected periodic orbits.

c_r through $(0, \pi)$, collide simultaneously with the boundary $x = 0$. However, $f_2(x)$ does not fulfil the conditions of theorem 2 as the eigenvalues associated with both fixed points are both positive.

As mentioned in the introduction, this situation leads to the so-called period adding big bang bifurcation and the orbits are organized by a Farey-tree-like structure. That is, near the big bang bifurcation, there exist an infinite number of bifurcation curves separating existence regions of different periodic orbits in such a way that, in between two regions, there exists another region locating a unique periodic orbit obtained by 'gluing' them and thus having a period which results from the addition of the periods of those. This implies that between two different bifurcation curves there exist an infinite number of them (see for example [1] for an extended explanation). This is shown in figure 8 by the one-dimensional bifurcation diagram along the curve shown in figure 7(*a*).

From the global overview of the bifurcation scenario shown in figure 7(*a*) it seems that all the bifurcation curves created at $(0, \pi)$ disappear at the intersection points of the curves $\xi^d_{\mathcal{RL}^n}$ and $\xi^c_{\mathcal{RL}^{n+1}}$. However, as we will immediately show, this cannot be the case.

Let us take a closer look for example at the point labelled with A in figure 7(*a*) whose surrounding is magnified in figure 9(*a*). As this point is given by the intersection of the curves $\xi^c_{\mathcal{RL}^2}$ and $\xi^d_{\mathcal{RL}}$, it represents the simultaneous collision of the periodic orbits $\underline{\mathcal{RL}^2}$ and $\underline{\mathcal{RL}}$ with the boundary. Therefore, the composite map

$$f_3(x) = \begin{cases} f_\ell f_r f_\ell(x) & \text{if } x \leqslant 0, \\ f_\ell f_r(x) & \text{if } x > 0 \end{cases} \tag{20}$$

possesses two fixed points colliding with the boundary $x = 0$ at the point A. The coordinates of A can be calculated solving the equations

$$f_\ell f_r f_\ell(0) = 0,$$
$$f_\ell f_r(0) = 0,$$

which leads to $A = (c^A_\ell, c^A_r) \simeq (0.883\,25, 1.377\,59)$.

One could also consider the iterated functions $f_r f_\ell f_\ell$ and $f_\ell f_\ell f_r$ for the left branch. However, one can see that the first option is the proper way of writing the corresponding iterate, as it collapses the corresponding periodic orbit of (18) to that fixed point of the third iterate which collides with the boundary $x = 0$ at the point A.

Expanding the gaps and the slopes of each branch of $f_3(x)$ at the discontinuity near A, one has

$$f_\ell f_r f_\ell(0)(\tilde{c}_\ell, \tilde{c}_r) \simeq 1.05483\tilde{c}_\ell + 0.17280\tilde{c}_r + O(\tilde{c}_\ell^2, \tilde{c}_r^2, \tilde{c}_\ell\tilde{c}_r), \tag{21}$$

$$(f_\ell f_r f_\ell)'(0)(\tilde{c}_\ell, \tilde{c}_r) \simeq 0.04935 + 0.01994\tilde{c}_\ell + 0.25224\tilde{c}_r + O(\tilde{c}_\ell^2, \tilde{c}_r^2, \tilde{c}_\ell\tilde{c}_r), \tag{22}$$

$$f_\ell f_r(0)(\tilde{c}_\ell, \tilde{c}_r) \simeq \tilde{c}_\ell - 0.17280\tilde{c}_r + O(\tilde{c}_r^2), \tag{23}$$

$$(f_\ell f_r)'(0)(\tilde{c}_\ell, \tilde{c}_r) \simeq -0.086401 + 0.44162\tilde{c}_r + O(\tilde{c}_r^2), \tag{24}$$

where $\tilde{c}_\ell = c_\ell - c_\ell^A$ and $\tilde{c}_r = c_r - c_r^A$. From equations (21) and (23), it is clear that there exist two directions in the parameter space (presented in figure 9(*a*) as two dotted straight lines) along which the position of the fixed points with respect to the boundary (the offsets at the origin) can be locally varied independently. This means that the re-parametrization

$$\hat{c}_\ell := f_\ell f_r f_\ell(0) = 1.05483\tilde{c}_\ell + 0.17280\tilde{c}_r + \text{h.o.t.}$$
$$\hat{c}_r := f_\ell f_r(0) = \tilde{c}_\ell - 0.17280\tilde{c}_r + \text{h.o.t.}$$

writes f_3 in the form of equation (1) fulfilling C.1. In addition, it comes from equations (22) and (24) that conditions C.2 and C.3 are also fulfilled: the colliding fixed points of (20) are stable and have associated eigenvalues of different signs. As a consequence, theorem 2 applies to f_3 and, therefore, the point A represents a big bang bifurcation of the incrementing type for the original map (18).

As the colliding fixed points of (20) with positive associated eigenvalue is $\underline{\mathcal{L}}$, the periodic orbits undergoing the incrementing scenario for f_3 are of the form $\underline{\mathcal{RL}^n}$. This implies that the periodic orbits for the original map (18) emerging at the point A are of type $\underline{\mathcal{RL}(\mathcal{RL}^2)^n}$, which are shift-equivalent to $\underline{\mathcal{LR}(\mathcal{LRL})^n}$ (see definition 3). This is shown in figure 9(*b*) where a one-dimensional bifurcation diagram is performed along the corresponding segment labelled in figure 9(*a*). As the coexistence regions between the periodic orbits of type $\underline{\mathcal{RL}(\mathcal{RL}^2)^n}$ and $\underline{\mathcal{RL}(\mathcal{RL}^2)^{n+1}}$ cannot be observed there, a magnification for the case $n = 2$ is shown in figure 9(*c*).

However, the question arises: where do all other border collision bifurcation curves created at $(0, \pi)$ end? As shown in figure 9(*d*), when moving away from A, there exists a point between the two segments labelled in figure 9(*a*) where the coexistence shown in figure 9(*c*) disappears. This point is given by the intersection of the corresponding curves $\xi^c_{\mathcal{RL}(\mathcal{RL}^2)^3}$ and $\xi^d_{\mathcal{RL}(\mathcal{RL}^2)^2}$ exactly as happened at the point A with the curves $\xi^c_{\mathcal{RL}^2}$ and $\xi^d_{\mathcal{RL}}$. Such a point would be the analogous to the one given by the intersection of the curves $\xi^c_{\mathcal{RL}(\mathcal{RL}^2)}$ and $\xi^d_{\mathcal{RL}}$ labelled with B in figure 9(*a*). This self-similarity suggests that this process takes place for every border collision curve, so forming an infinite tree of big bang bifurcations of period incrementing type whose mother node is the point $(0, 0)$, generating the complete period adding structure absorbed by the point $(0, \pi)$.

5.2. Example 2

Let us now consider a second example fulfilling conditions C.1″–C.3″ (and C.1–C.3)

$$f(x) = \begin{cases} c_\ell + \frac{2}{5}x(x+2) =: f_\ell(x) & \text{if } x \leqslant 0, \\ -c_r + \frac{1}{2}x(x-1) =: f_r(x) & \text{if } x > 0, \end{cases} \tag{25}$$

which is shown in figure 10(*a*).

As expected, the origin of the parameter space $c_\ell \times c_r$, presented in figure 10(*b*), is a big bang bifurcation point of the period incrementing type. Moreover, arguing exactly as before,

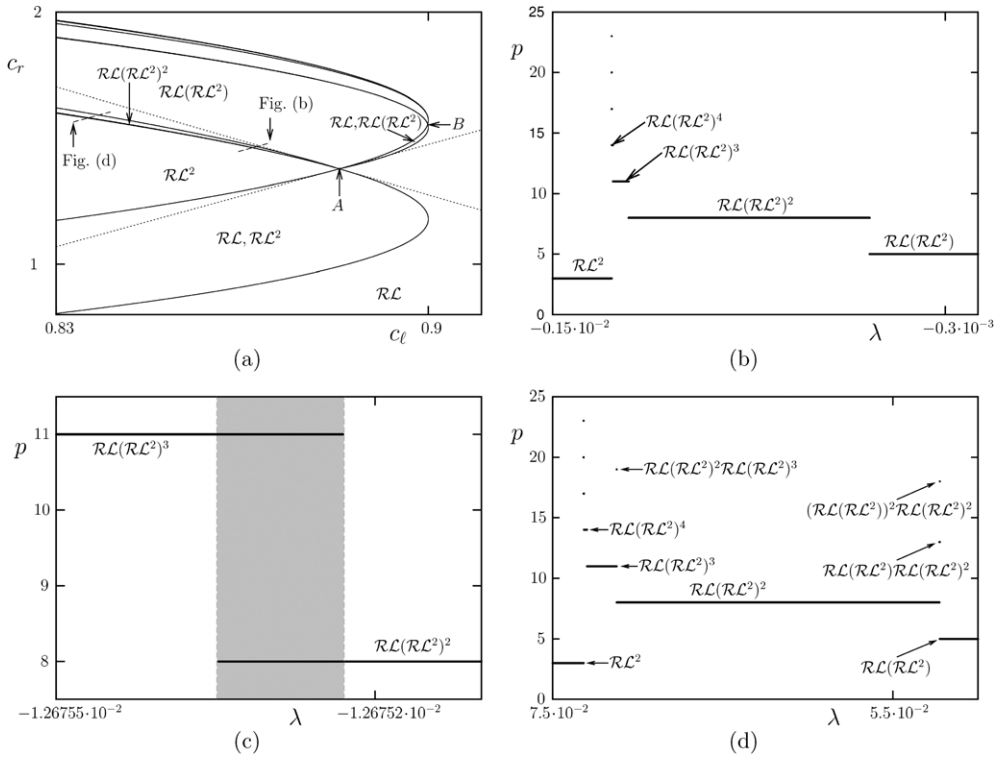

Figure 9. Bifurcation scenario near the point A (see figure 7(a)). (a) Blow up labelled in figure 7(a). The two dotted straight lines are the directions along which the right and left images of 0 by $f_3(x)$ remain (locally) constant. (b) One-dimensional bifurcation diagram along the segment labelled in (a) period incrementing scenario. (c) Magnification of the coexistence (grey region) between the periodic orbits $\mathcal{RL}(\mathcal{RL}^2)^2$ and $\mathcal{RL}(\mathcal{RL}^2)^3$ shown in (b). (d) Bifurcation diagram along the segment labelled (d) in figure 9(a); far enough from A, the period incrementing structure generated at A disappears.

one can show that the situation between the points (0, 2) and (0, 0) is the same as in the previous example between $(0, \pi)$ and (0, 0). This has been validated with numerical simulations which we do not show as they are equivalent to the ones presented in figures 7(b), (c), (d) and 8. Therefore we omit further comments in that direction.

However, there exists in the c_ℓ axis of figure 10(b) several points that deserve special interest. For example, let us consider the point $(1, 0)$. As one can see in figure 10(b), this point is given by the collision of the bifurcation curves $\xi^d_{\mathcal{R}}$ (the horizontal axis) and $\xi^c_{\mathcal{RL}}$, where the fixed point $\underline{\mathcal{R}}$ and the periodic orbit $\underline{\mathcal{RL}}$ simultaneously collide with the boundary. Therefore, after re-parametrization along proper directions in the parameter space[8], the map

$$f_2(x) = \begin{cases} f_r f_\ell(x) & \text{if } x \leqslant 0, \\ f_r(x) & \text{if } x > 0 \end{cases} \tag{26}$$

can be written as in (1) fulfilling C.1. As before, as the colliding periodic orbits are stable and their associated eigenvalues have the proper signs, conditions C.2 and C.3 are also fulfilled. Therefore, theorem 2 applies and the point $(1, 0)$ represents a big bang bifurcation of period

[8] We skip the details as one has just to proceed as in example 1.

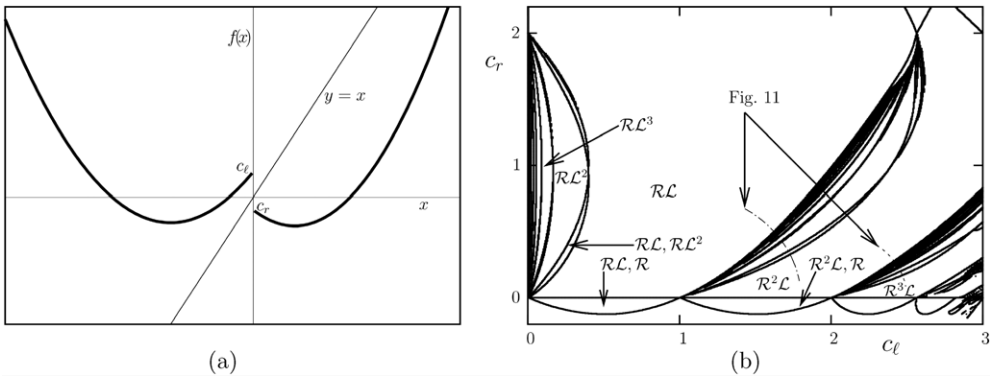

Figure 10. (*a*) System function of example 2 defined in equation (25). (*b*) Border collision bifurcation curves of example 2.

incrementing type. As the periodic orbit with positive associated eigenvalue is $\underline{\mathcal{RL}}$, the periodic orbits of the original map, (25), emerging at $(1, 0)$ are of type $\underline{\mathcal{R}(\mathcal{RL})^n}$. This is shown in figures 11(*a*) and (*b*) through the one-dimensional bifurcation diagram along the curve labelled in figure 10(*b*).

One can proceed analogously and show that the situation is repeated for the other points, $(p_n, 0)$, also located at the horizontal axis of figure 10(*b*).

In order to show that, let us consider the equation

$$f_r^n f_\ell(0) = f_r(0), \qquad c_r = 0 \tag{27}$$

and let p_n be the root of equation (27) which is not a root of the same equation using $n - 1$ instead of n. Then, one can easily see that the map

$$f_n(x) = \begin{cases} f_r^n f_\ell(x) & \text{if } x \leqslant 0, \\ f_r(x) & \text{if } x > 0 \end{cases} \tag{28}$$

possesses two colliding fixed points (is continuous at $(c_\ell, c_r) = (p_n, 0)$). Again, under proper re-parametrization, it can be written in the form of (1) and conditions C.1–C.3 hold at $(c_\ell, c_r) = (p_n, 0)$. Therefore, for every $(p_n, 0)$ there exists an arbitrarily small open set containing that point such that only periodic orbits of type $\underline{\mathcal{R}(\mathcal{R}^n\mathcal{L})^m}$ exist for all $m \geqslant 0$. Moreover, there exist regions in that open set where two $\underline{\mathcal{R}(\mathcal{R}^n\mathcal{L})^m}$ and $\underline{\mathcal{R}(\mathcal{R}^n\mathcal{L})^{m+1}}$ orbits coexist $\forall m \geqslant 0$.

6. Conclusions

Big bang bifurcations occur in low-dimensional piecewise-smooth systems typically whenever two fixed points cross simultaneously the boundary and become virtual. This is given by a transverse intersection between two border collision bifurcation curves when the considered parameters control the distance between the boundary and the fixed points.

So far we have presented this situation for the one-dimensional case for which the boundary is represented by a single point ($x = 0$) where the map has a jump discontinuity. By theorem 2, we have explicitly and rigorously characterized the infinite number of periodic orbits that appear after the collision of two fixed points with the boundary when they are attracting (the map is locally contractive) and have associated eigenvalues of opposite sign: a big bang bifurcation of periodic incrementing type occurs. As mentioned in remark 7, in the case that the branch

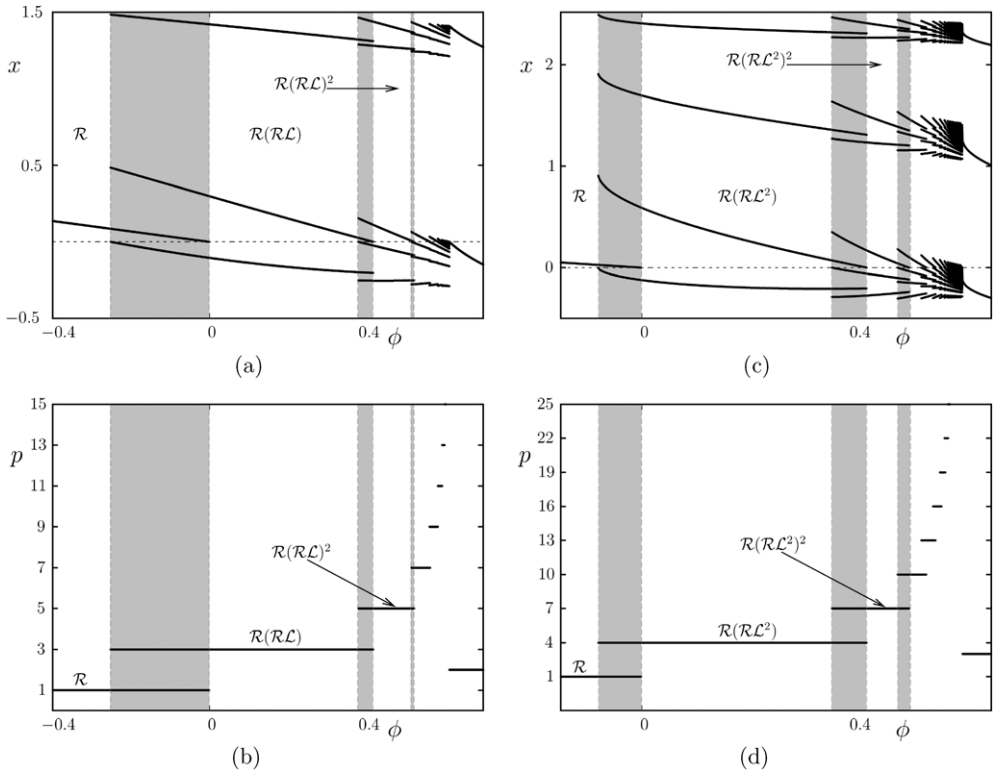

Figure 11. Bifurcation structure around the big bang bifurcation points at $(c_\ell, c_r) = (1, 0)$ ((*a*) and (*b*)) and $(c_\ell, c_r) = (p_2, 0)$ ((*c*) and (*d*)). (*a*) and (*c*) Bifurcation diagram along the curves labelled in figure 10(*b*). (*b*) and (*d*) Periods of the periodic orbits. The grey regions indicate coexistence between two periodic orbits.

corresponding to the fixed point with negative associated eigenvalue is replaced by a constant function in an open set containing $x = 0$, the bifurcation scenario remains the same except that the coexistence regions disappear, and a big bang of the so-called pure incrementing type occurs.

We have also given examples showing that one can consider a proper renormalization of the map in order to study other big bang bifurcations in the parameter space. In the same examples we have also checked the result conjectured in the introduction; that is, when both eigenvalues of the colliding fixed points are positive, then the so-called period adding big bang bifurcation takes place. A proof of that is left for future work. Using also renormalization arguments we have suggested that the bifurcation curves issuing from the detected period adding big bang bifurcation are 'collected' by an infinite cascade of period incrementing big bang bifurcations. A rigorous and more detailed study of this situation will be reported elsewhere.

Acknowledgments

The authors would like to thank DAAD–'La Caixa' grant program and the German Research Foundation (DFG) for partially supporting this work.

References

[1] Avrutin V and Schanz M 2006 On multi-parametric bifurcations in a scalar piecewise-linear map *Nonlinearity* **19** 531–52

[2] Avrutin V, Schanz M and Banerjee S 2006 Multi-parametric bifurcations in a piecewise-linear discontinuous map *Nonlinearity* **19** 1875–906

[3] Avrutin V, Schanz M and Banerjee S 2007 Codimension-3 bifurcations: explanation of the complex 1-, 2- and 3D bifurcation structures in nonsmooth maps *Phys. Rev.* E **75** 066205

[4] Leonov N N 1959 On a pointwise mapping of a line into itself *Radiofisika* **2** 942–56 (in Russian)

[5] Mira C 1987 *Chaotic Dynamics: From the One-Dimensional Endomorphism to the Two-Dimensional Diffeomorphism* (Singapore: World Scientific)

[6] Coullet P C, Gambaudo J M and Tresser C 1984 Une nouvelle bifurcation de codimension 2: le colage de cycles *C. R. Acad. Sci., Paris I* **299** 253–6

[7] Gambaudo J M, Glendinning P and Tresser C 1984 Collage de cycles et suites de Farey *C. R. Acad. Sci., Paris I* **299** 711–4

[8] Gambaudo J M, Glendinning P and Tresser T 1988 The gluing bifurcation: symbolic dynamics of the closed curves *Nonlinearity* **1** 203–14

[9] Gambaudo J M, Procaccia I, Thomae S and Tresser C 1986 New universal scenarios for the onset of chaos in Lorenz-type flows *Phys. Rev. Lett* **57** 925–8

[10] Ghrist R and Holmes P J 1994 Knotting within the gluing bifurcation *IUTAM Symp. on Nonlinearilty and Chaos in the Enginnering Dynamics* ed J Thompson and S Bishop (New York: Wiley) pp 299–315

[11] Homburg A J 1996 Global aspects of homoclinic bifurcations of vector fields *Mem. Am. Math. Soc.* **121** (578) (special issue)

[12] Lyubimov D V, Pikovsky A S and Zaks M A 1989 *Universal Scenarios of Transitions to Chaos via Homoclinic Bifurcations* (*Mathematical Physics Review* vol 8) (London: Harwood Academic) (Russian version 1986 as a Preprint (192) of Russian Academy of Science, Institute of Mechanics of Solid Matter, Sverdlovsk)

[13] Turaev D V and Shil'nikov L P 1987 On bifurcations of a homoclinic 'figure of eight' for a saddle with a negative saddle value *Sov. Math. Dokl.* **34** 397–401 (Russian version 1986)

[14] Procaccia I, Thomae S and Tresser C 1987 First-return maps as a unified renormalization scheme for dynamical systems *Phys. Rev.* A **35** 1884–900

[15] Sparrow C 1982 *The Lorenz Equations: Bifurcations, Chaos, and Strange Attractors* (Berlin: Springer)

[16] Gambaudo J and Tresser C 1988 On the dynamics of quasi-contractions *Bol. Soc. Bras. Mat.* **19** 61–114

[17] Alsedà Ll and Falcó A 2003 On the topological dynamics and phase-locking renormalization of Lorenz-like maps *Ann. Inst. Fourier* **53** 859–83

[18] Alsedà Ll and Llibre J 1989 Kneading theory of Lorenz maps *Dyn. Syst. Ergod. Theory* **23** 83–9

[19] Alsedà Ll, Llibre J, Misiurewicz M and Tresser C 1989 Periods and entropy for Lorenz-like maps *Ann. Inst. Fourier (Grenoble)* **39** 929–52

[20] Glendinning P 1990 Topological conjugation of Lorenz maps to β-transformations *Math. Proc. Camb. Phil. Soc.* **107** 401–13

[21] Hubbard J H and Sparrow C T 1990 The classification of topologically expansive Lorenz maps *Commun. Pure Appl. Math.* **43** 431–43

[22] Labarca R and Moreira C 2001 Bifurcation on the essential dynamics of Lorenz maps and applications to Lorenz-like flows: contributions to study of expanding case *Bol. Soc. Bras. Mat.* **32** 107–44

[23] Labarca R and Moreira C 2006 Essential dynamics for Lorenz maps on the real line and the lexicographical world *Ann. Inst. Henri. Poincaré Anal. Non Linéaire* **23** 683–94

[24] di Bernardo M, Budd C J, Champneys A R and Kowalczyk P 2008 *Piecewise-smooth Dynamical Systems: Theory and Applications* (*Applied Mathematical Sciences* vol 163) (Berlin: Springer)